

VISdish: A new tool for canting and shape-measuring solar-dish facets

Marco Montecchi, Giuseppe Cara, and Arcangelo Benedetti

Citation: *Review of Scientific Instruments* **88**, 065107 (2017); doi: 10.1063/1.4984944

View online: <http://dx.doi.org/10.1063/1.4984944>

View Table of Contents: <http://aip.scitation.org/toc/rsi/88/6>

Published by the American Institute of Physics



VISdish: A new tool for canting and shape-measuring solar-dish facets

Marco Montecchi,^{a)} Giuseppe Cara, and Arcangelo Benedetti
Department of Energy Technologies, ENEA, S. Maria di Galeria, Roma 00123, Italy

(Received 16 January 2017; accepted 20 May 2017; published online 9 June 2017)

Solar dishes allow us to obtain highly concentrated solar fluxes used to produce electricity or feed thermal processes/storage. For practical reasons, the reflecting surface is composed by a number of facets. After the dish assembly, facet-canting is an important task for improving the concentration of solar radiation around the focus-point, as well as the capture ratio at the receiver placed there. Finally, flux profile should be measured or evaluated to verify the concentration quality. All these tasks can be achieved by the new tool we developed at ENEA, named VISdish. The instrument is based on the visual inspection system (VIS) approach and can work in two functionalities: canting and shape-measurement. The shape data are entered in a simulation software for evaluating the flux profile and concentration quality. With respect to prior methods, VISdish offers several advantages: (i) simpler data processing, because light point-source and its reflections are univocally related, (ii) higher accuracy. The instrument functionality is illustrated through the preliminary experimental results obtained on the dish recently installed in ENEA-Casaccia in the framework of the E.U. project OMSoP. *Published by AIP Publishing.* [<http://dx.doi.org/10.1063/1.4984944>]

I. INTRODUCTION

Dishes are one of the four main typologies of concentrating solar power (CSP) plants,¹ with the remarkable characteristic of offering high solar concentration at quite limited power. Although the instantaneous electricity production via Stirling motors is their most known application, the Solar Thermal Electricity Global Outlook 2016² considers that technology as not appropriate for utility scale applications. Therefore new approaches like direct steam generation,³ chemical reaction,⁴ and thermochemical storage⁵ are under investigation. Recently, the underway E.U. project Optimised Microturbine Solar Power system (OMSoP)⁶ aims to evaluate the feasibility of replacing Stirling motors with micro gas-turbines, which are expected to exhibit a longer maintenance-free operating period. The demonstrative OMSoP dish has been designed and realized by INNOVA and was installed in the ENEA-Casaccia site. The need to check and improve its optical performances promoted us to develop a suitable method and instrument. This paper describes the outlined instrument named VISdish and shows its functionality through the preliminary experimental results obtained for the OMSoP dish.

II. VISUAL INSPECTION SYSTEM APPROACH

About ten years ago, we outlined the Visual Inspection System (VIS) approach, based on the idea of placing a source nearby the focus of parabolic-trough systems and acquiring a number of images in the near-field from different positions.⁷ On the basis of the VIS approach, we developed the following instruments: (1) VISfield to verify the mutual optical alignment between the receiver tube and the parabolic trough reflector for modules in the field;⁸ (2) VISSHED, the adaptation

of VISfield for the quality control in the shed, soon after the module assembling;⁹ and (3) VISprofile for the shape measurement of parabolic-trough facets in laboratory/industry.¹⁰ All these instruments are currently marketed by MARPOSS under ENEA's license.

Now we once again benefited of the VIS approach and outlined the simple instrument named VISdish, sketched in Fig. 1. It is composed by a LCD monitor showing the point-source $S(x_s, y_s, f)$ and the observer $V(0, 0, d)$ placed along the dish axis at distance d from the vertex. The observer V sees the source S reflected on the point $P(x, y, z)$ if the normal vector in P lies in the plane formed by the incident and the reflected rays and bisects the angle they form, according to reflection's law. This fact can be used to accomplish the two tasks, facet-canting and shape-measurement, needed for the optical characterization of the dish.

A. Facet canting by VISdish

Concerning the facet canting, let S be a point source in the focal plane with coordinates (x_s, y_s, f) such that the ray hitting the point P of the ideal paraboloid is reflected towards V. The observer V sees the source S reflected on P. When P is the central point of a given real facet, that features can be used to drive the canting operation: the panel alignment is adjusted until the observer V sees S imaged on P.

Generally speaking, because the paraboloid has only two optically conjugated points (f with $+\infty$), the canting of each facet needs a specific position of the point source S in the LCD monitor. The ensemble of these points appears distributed around the optical axis like the caustic predicted for the OMSoP dish and is shown in Fig. 2(a). This figure is obtained by tracing the ray from V to one of the central points of the 40 facets composing the reflector of the OMSoP dish, computing the reflected ray, and its intersection with the plane $z=f$, where f is set to the OMSoP design value, 7040 mm. On the other

^{a)}Electronic mail: marco.montecchi@enea.it

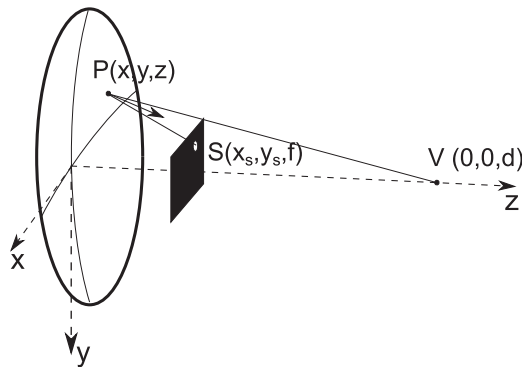


FIG. 1. Concept of the VIS method applied to dishes.

hand, when the observation distance is much greater than the focal length, one can optimize the distance of the LCD monitor to see that these S points almost collapsed in a unique dot. As an example in the case of the OMSoP dish, for logistic reasons, the observer V can be hosted in a building of ENEA-Casaccia at $d = 320$ m. As shown in Fig. 2(b), the caustic on the plane $d = 7230$ mm almost collapses in a unique point. That allows us to greatly simplify the canting procedure by using a unique point-source displayed by a fake-monitor as will be shown in Sec. III B. The optimal size of that point-source depends on the shape quality of the facet: higher the quality, smaller its diameter. It should be set in such a way that the observer never sees the facet surface completely illuminated by the source.

A human observer placed in V can easily guide the facet-canting process by keeping in mind the simple criterion of maximization of the area of the facet surface reflecting the point-source; the needed adjustments are identical to those to make a plane horizontal by means of a bull's eye spirit level. Of course the human observer could be replaced by a camera with remote access from the operator who is adjusting the facet orientation, or even the whole canting process could be fully automatized by means of a suitable image processing that drives some actuators acting on the fixing points of the facet.

The VISdish-canting method reminds the color look-back alignment approach proposed by Andraka *et al.*¹¹ but differs for using a unique colored spot, centered on the paraboloid

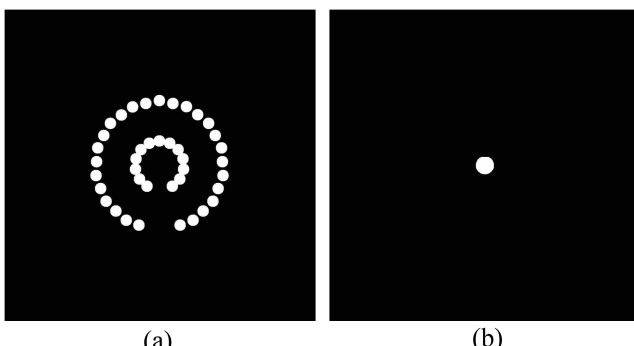


FIG. 2. Caustic on $z = f = 7040$ mm (a) and $z = 7230$ mm (b) for a point source placed in $V = (0, 0, 320)$ m and considering the only rays reflected in the central points of the 40 facets composing the reflector of the OMSoP dish.

axes, instead of a multi-color structured target. Such a simplification is allowed by positioning the single spot (point source) along the dish axes, a bit farther than the focus (for OMSoP dish, about 20 cm), where the caustic almost collapses in a unique point (see Fig. 2(b)). To do that, the receiver should not be installed. That drawback is repaid by the simplicity, avoiding the problem of identifying the proper segment of the structured target for the given facet. In principle, canting could be contemporaneously conducted on all facets, without the need of any image processing, but only keeping in mind the bull's eye criterion.

B. Shape measurement by VISdish

Considering Fig. 1, on the basis of the reflection's law, the experimental value of the unit vector \mathbf{n}_{exp} normal to the dish surface in P is given by

$$\mathbf{n}_{exp} = \frac{\vec{PS}/|\vec{PS}| + \vec{PV}/|\vec{PV}|}{|\vec{PS}/|\vec{PS}| + \vec{PV}/|\vec{PV}||}, \quad (1)$$

where the position of S is known, V is kept fixed in $(0, 0, d)$ and the real world coordinates of P are evaluated by the raw-column indices i, j and i_0, j_0 , respectively, of P and the dish-center in the digital image acquired from V ,

$$x = c(i - i_0), \quad y = c(j - j_0), \quad (2)$$

where c is the scale factor connecting the image to the real world; c can be evaluated by the ratio between the real diameter of the dish to its pixel-value in the image,

$$c = \frac{\varnothing}{\varnothing_{px}}. \quad (3)$$

That procedure requires high quality lenses, otherwise the images should be corrected by the characteristic matrix and distortion coefficients of the camera.¹² Moreover, thanks to $d \gg f$, the parallaxes error can be neglected; as an example for the OMSoP dish, in the worst case (along the external rim) such an error is lower than 0.1 mm. Finally the coordinate z of P is set to the design value

$$z = \frac{x^2 + y^2}{4f}. \quad (4)$$

Differently from facet-canting, slope-measurement certainly requires a real monitor properly sized to see from V the reflection of S spanning, sooner or later, the whole dish-surface. More precisely, S is successively displayed at a number of different positions on the LCD monitor, and for each one, an image is acquired from V . As a general rule, the lower the shape-quality, the larger the minimal size of the monitor needed for sampling the whole dish-surface. A simple check to verify the proper monitor sizing is to display all its pixels in white: the size is sufficient if from V the whole dish surface appears enlightened.

Even if not mandatory, for the sake of cheapness, the optimal position of the LCD monitor is where the caustic size is minimal. For the OMSoP dish, such value is $z = 7230$ mm when the observer V is in $(0, 0, 320)$ m.

The measurement time is dramatically reduced by displaying one single strip (vertical or horizontal) instead of

one single-point. Let N be the step-number per dimension, the number of needed images is $2N$ (N horizontal + N vertical, for strip-source) instead of $N \times N$ (for point-source). The data-processing analyses the whole set of acquired images searching for the couple of vertical and horizontal stripes for which the considered pixel centered in P appears brighter; their vertical and horizontal coordinates correspond to the position of the point-source under which the observer V sees the point P enlightened. Then the unit vector \mathbf{n}_{exp} is computed by Eq. (1). This process is repeated for each pixel composing the image of the dish-surface.

Hardware and slope-computing of VISdish remind AIMFAST,¹³ but the underlying approaches are quite different: VIS and Fringe Reflection Technique (FRT),¹⁴ respectively. In VIS, the source-position is well defined, while in FRT given P , it must be inferred by analyzing a number of different patterns. As a general rule, the more the reflecting surface is uneven, the greater the number of different patterns needed to identify the part illuminating P from the observer V ; such number must be evaluated for each specific case. In comparison, the VIS method needs to process a larger number of images, but with a much simpler algorithm always giving unambiguous results, and over a reduced amount of pixels composing the image (those with grey level over threshold).

The deviation of the experimental slope from the design value is given by three different quantities: the magnitude of the slope-deviation

$$\Delta_{slope} = \arccos(\mathbf{n}_{exp} \cdot \mathbf{n}_{ideal}) \quad (5)$$

and the deviations along the x and y axes

$$\Delta_{slopeX} = \arctan \frac{\partial z}{\partial x_{exp}} - \arctan \frac{x}{2f} \quad (6)$$

$$\Delta_{slopeY} = \arctan \frac{\partial z}{\partial y_{exp}} - \arctan \frac{y}{2f}, \quad (7)$$

being $\frac{\partial z}{\partial x} = \frac{x}{2f}$ and $\frac{\partial z}{\partial y} = \frac{y}{2f}$ the design values.

Concerning the accuracy, the alignment error of the observer V along the dish optical axis returns as a systematic error and can be easily removed by setting a proper pointing-bias which minimizes the mean value of the slope deviation along the x and y axes over the dish surface. With the help of a total station, the monitor can be easily aligned with accuracy better than 1 mm, which once again affects the results with a systematic error. In conclusion, the accuracy on the slope is essentially driven by the half-ratio strip-thickness to length of the optical path from the monitor to the dish.

III. RESULTS

A. Geometrical characterization

The OMSoP dish does not belong to an industrial series; it is a prototype without reference points for the identification of the vertex and axis of the design paraboloid. Therefore the dish geometrical characterization was the very first step of our on-field activity. It was accomplished by two different techniques: photogrammetry and total-station measurements. Both give the 3D coordinates of some selected points.

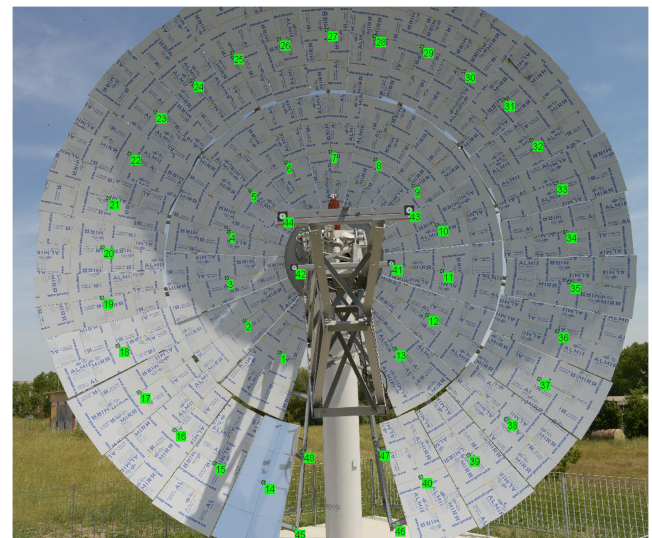


FIG. 3. Arrangement of the targets used for the preliminary geometrical characterization by photogrammetry.

Photogrammetry requires the arrangement of a suitable number of targets on the object to be measured; then several photos are acquired from different points of view. In our case, as shown in Fig. 3, we affixed one target in the central point of each one of the 40 facets (mirror panels) composing the reflector (targets 1-40). These were temporary points successively lost with the removal of the facet protective film. Other 4 targets (41-44) are permanent and were affixed along the receiver bearing structure; further 4 permanent targets (45-48) are on the two ribs not covered by the facets (see Fig. 3).

The coordinates of the targets 1-40 have been processed to locate the natural coordinate-system (shown in Fig. 1) where the paraboloid reflecting surface is given by Eq. (4); the focal length was set to the design value $f = 7040$ mm. From here on, the paraboloid axis is set to the z axis of that coordinate-system.

The remaining points 41-48 are permanent and were also measured by the total station (Leica TDA 5005) in order to compose a set of reference points that can be used at any time to locate the vertex and axis of the paraboloid.

In order to apply the canting procedure described in Sec. II A, the observer eye V must lie on the paraboloid axis. At that purpose, as shown in Fig. 4, a couple of front and rear sights have been placed on the dish with the help of the total station: a red dot is installed at the end of the rod hung on the right of the fake-monitor; the projection of the red dot along the z axis is marked close to the $z = 0$ mm plane by the black cross-hair drawn on the drum. The dish aiming is adjusted until the observer V sees the red dot sighted with the black cross-hair. Then from this sighting axis, the remote observer V must shift himself for a known amount (84 mm downwards and 914 mm to the left), to be exactly positioned along the optical z axis of the paraboloid. We evaluated the aim accuracy of this method as better than 0.1 mrad.

B. Canting

As shown in Fig. 5, a fake-monitor displaying a red spot on a black background was installed on the bearing-structure on the plane $z = 7230$ mm and centered in $(0, 0, 7230)$ mm. The

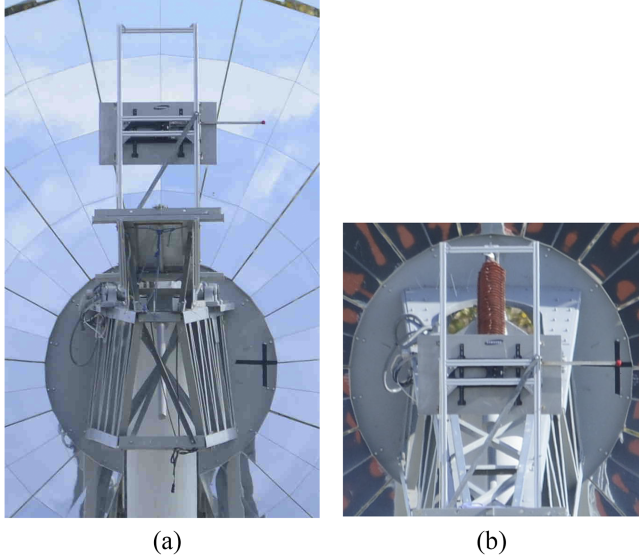


FIG. 4. Front (the red dot on the right of the fake-monitor) and rear (the cross-hair drawn on the dish drum) sights used to aim the dish towards the observer (a). When the observer placed in V sees the front sight superimposed to the rear sight (b), his eye is crossed by the straight line passing by the two sights; this straight line is parallel to the paraboloid axis. From this position, the observer must shift himself for a known amount to be exactly positioned along the z axis.

spot has a diameter of 120 mm (a bit less than the design value of the receiver-window, 150 mm) and is painted red to ensure a good visibility even in daylight conditions.

The execution of the facet-canting procedure described in Sec. II A has taken a couple of days. Initially the great part of the facets resulted strongly misaligned. After one day, as shown in Fig. 6, only a few facets remained misaligned. At the end of the canting, a large part of the dish area appears red-colored; the remaining part is essentially black, and only a small fraction is bright, meaning large imperfections of the mirror shape so that the observer views the sky instead of the fake monitor. Taking into account that for the ideal parabolic reflector, the entire surface should appear red-colored, the final result clearly indicates the limited quality of the facet-shape.



FIG. 5. Fake-monitor displaying a red dot on black background.



FIG. 6. Facet canting by VISdish after one day.

Noteworthy, most of the time was spent to place the operator (in an aerial platform, back parked) in a useful position such that he could operate on the specific facet. Then the alignment took only about 1 min per facet.

C. Shape

The shape of the OMSop dish was investigated with a consumer LCD 16:9 44 " monitor, with resolution 1920×1080 pixels, placed at $z = 7230$ mm (see Sec. II B). As shown in Fig. 7, unfortunately the monitor-size seems not large enough to allow the measurement over the whole paraboloid: the monitor surface is entirely bright, but a small fraction of the dish surface does not reflect it and therefore cannot be sampled.

The VISdish measurement was accomplished nightly because the monitor brightness was not sufficient to properly discriminate the brightness due to the monitor from that caused

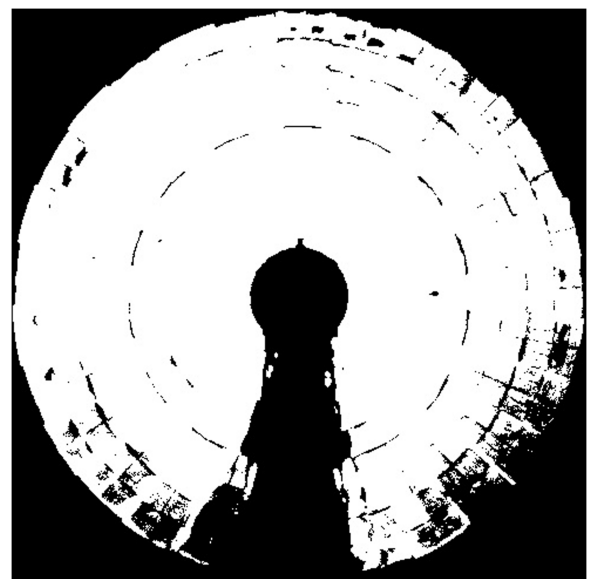


FIG. 7. Map of the successfully measured pixels (white).

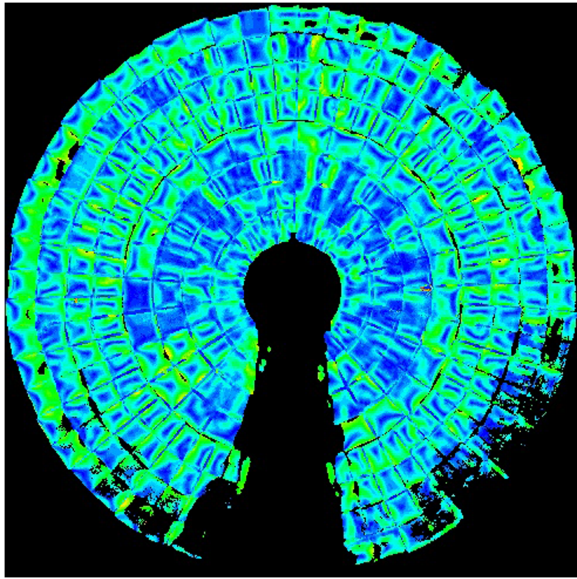


FIG. 8. Contour map of the experimental magnitude of the slope-deviation Δ_{slope} . Black = not sampled, pixel-color from blue to red corresponds to the slope-deviation from 0 to 20 mrad.

by the environment. That discrimination is obtained by setting a suitable threshold value for the grey level: if above, the brightness is imputed to the white-strip displayed by the monitor. The minimal strip-thickness, ensuring a sufficient contrast between bright and dark, has been evaluated to 8 pixels with a 8-bit depth camera. Consequently the slope-accuracy is about 0.1 mrad but could be increased by adopting a camera with a higher bit-depth.

Figures 8 and 9 show the contour map and the distribution of the experimental magnitude of the slope-deviation, respectively. The distribution is peaked at 5 mrad and ranges from 0 to 20 mrad. The distributions of the slope-deviation along the x and y axes are shown in Fig. 10; they range in about ± 20 mrad.

The image-processing is dealt pixel by pixel, and the results are saved raw by raw in a textual file by reporting the

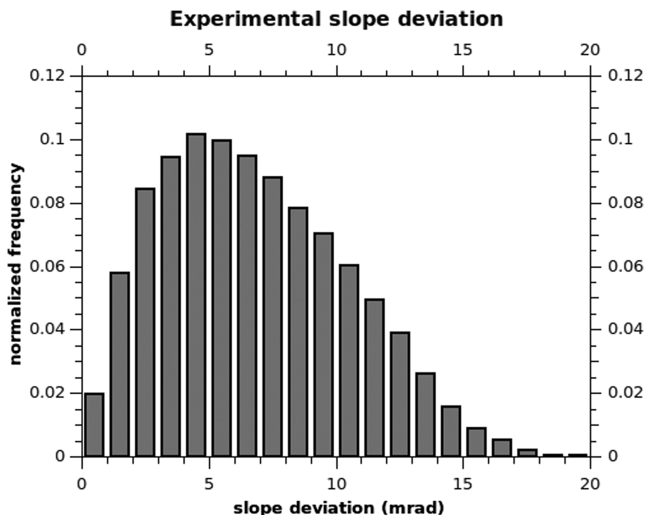


FIG. 9. Distribution of the slope-deviation magnitude.

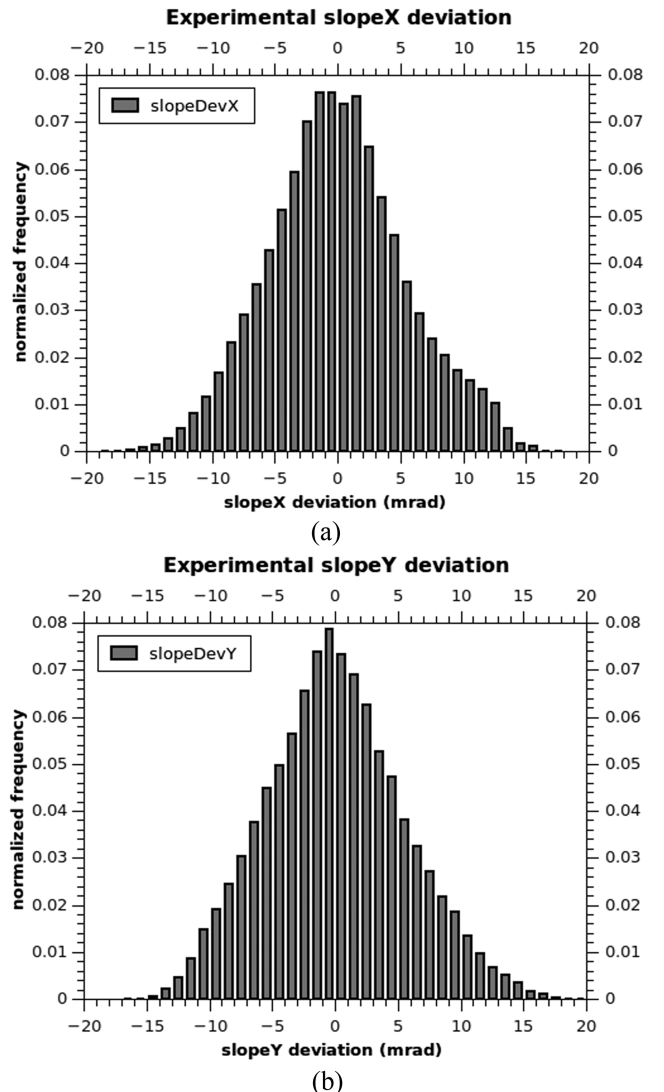


FIG. 10. Distribution of slope-deviation along x (a) and y (b) axes.

following value: $x, y, z, n_x, n_y, n_z, \Delta_{\text{slope}}, \Delta_{\text{slope}X}, \Delta_{\text{slope}Y}$, where $\mathbf{n}_{\text{exp}} = (n_x, n_y, n_z)$.

Noteworthy, one could evaluate the shape-height (z) by numerical integration of the partial derivatives, but the high segmentation of the facet surface together with the long observation distance makes the shape only slightly affecting the concentration effectiveness.

D. Flux prediction

The results obtained with the VISdish were entered in SIMULDISH, the software developed by ENEA for simulating the concentrated flux around the focal point of a dish. SIMULDISH considers the dish as perfectly tracking the Sun, and for each entered shape-data, it calculates the Sun Conic Reflectance $SCR(\theta_{\text{inc}}, \varphi)$ at the proper incidence angle θ_{inc} and over the φ range 0–20 mrad. The SCR concept was recently proposed¹⁵ to make the drafting easier, the guidelines for measuring the reflectance for CSP applications. More precisely, the SCR of some specimens of the solar mirror (ALMIRR 303) adopted for the OMSoP dish was experimentally measured

TABLE I. Main features of OMSop dish. The quantities marked with (*) are calculated for a circular receiver window with diameter 150 mm.

Effective reflecting area	83.25 m ²
Optimal z	7.02 m
Maximum concentration	1677 suns
Mean concentration (*)	1216 suns
Geometrical intercept factor (*)	0.310
Efficiency (*)	0.258

with the Solar Mirror Qualification setup.^{16,17} Also these data were entered in SIMULDISH.

SIMULDISH accurately predicts the reflected radiation, which is analyzed in the neighborhood of the focal point by a virtual stacked multi-CCD detector, orthogonal and centered to the z axis; each virtual CCD layer is lying at a different z level and measures the radiation without any disturbance (on it).

Noteworthy, another advantage of using SCR is the dramatic cut-down of the computing time: ray-tracing is limited to follow the ray coming from the center of the Sun for determining the impact point of its reflection on the virtual CCD; then the distribution of the solar radiation around the impact point is analytically calculated on the basis of SCR data.

At the end of the data processing, SIMULDISH allows evaluating many important features of the dish, the most important are summarized in Table I. The geometrical intercept factor for a circular receiver window with diameter 150 mm is maximum when the window is set at $z = 7.02$ m. Figure 11 shows the contour map of the flux on the plane $z = 7.02$ m.

For the practical purpose of capturing solar energy, the optical efficiency η is a very important parameter, relating the amount of power P_w entering the receiver-window with the available *DNI* and the effective reflecting area A,

$$P_w = \eta A DNI. \quad (8)$$

The optical efficiency of the OMSop dish is quite low, $\eta = 0.258$. This result can be understood by considering the slope-deviation magnitude measured with VISdish and is reported in Sec. III C: it is peaked at 5 mrad; therefore, after

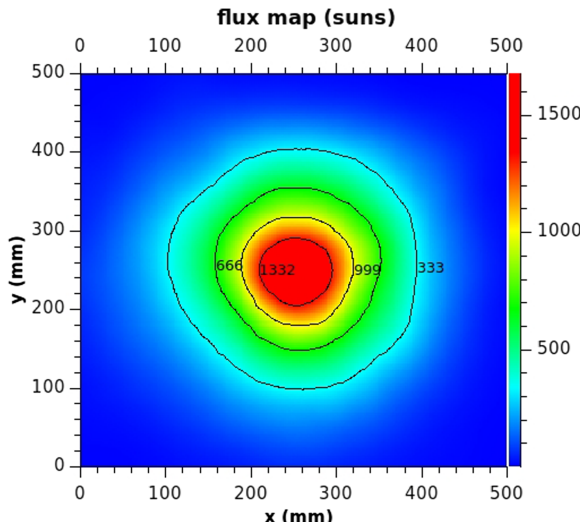


FIG. 11. Contour map of the flux on the plane $z = 7.02$ m.

7 m the reflected rays are displaced from the focal point of about 70 mm, which is very close to the radius of the circular receiver-window. Therefore a large amount of radiation does not enter the receiver-window.

Although the dish efficiency could be increased by enlarging the window diameter, one has to carefully balance that benefit with the higher radiance loss. On the basis of these results, the diameter of the OMSoP receiver was increased up to 220 mm and its design consequently refined.

In the future, we would like to improve the efficiency by replacing the facets with other much better shaped ones and made with a more efficient solar mirror.

IV. DISCUSSION

The visual inspection system method⁷ differs from the most known techniques¹⁸ for the characterization of CSP concentrators, like VSHOT, photogrammetry, and deflectometry for the following points, respectively: (i) VIS always adopt incoherent light sources; (ii) VIS does not need the apposition of targets; (iii) in VIS apparatus, the position of the optical source is always well known, with beneficial effect on accuracy.

The instrument herein described is just one of the several outlined on the basis of the VIS method. VISdish is conceived for canting and shape-measuring solar-dish facets; it is simply composed by a LCD monitor and an observer (camera), respectively, placed nearby the focus f and at distance $d \gg f$. The minimal-size constrain for the LCD monitor is less stringent at z where the dispersion of the caustic from the observer point is minimal; for the OMSoP dish and observation distance of 320 m, the optimal point from the vertex is about 20 cm farther than the focus.

Canting can be carried out in daylight by replacing the LCD monitor with a fake-monitor displaying a central colored spot on black background. The spot diameter should be set in such a way that the observer never sees the facet surface completely illuminated by the source; as general rule, higher the shape quality, smaller the spot diameter. From the observation point, canting is performed by the same method used for making a plane horizontal by means of a bull's eye spirit level; here the criterion is to maximize the area of the facet surface reflecting the colored spot.

With respect to the color look-back alignment approach,¹¹ VISdish uses a simpler colored spot, fine for canting all facets at the same time. In principle, canting could be contemporaneously performed on all facets, without the need of any image processing, but only keeping in mind the bull's eye criterion. Moreover, differently from the method proposed by Wang *et al.*,¹⁹ where the reflection of laser beam is analyzed, VISdish canting is driven by considering the whole facet surface, so that local shape-imperfections have low weight.

Concerning the second functionality (shape-measurement), in the case of the OMSoP dish, we found the nightly operation necessary, otherwise environmental lightning would surpass the one due to the LCD monitor brightness. Probably this limitation is only due to the quite large amount of diffuse reflectance exhibited by an ALMIRR 303 solar mirror (about

6% beyond 20 mrad) and may be impaired by adopting a less diffusive solar mirror.

With respect to AIMFAST,¹³ VISdish setup is cheaper and more simple. Conversely the number of images to be processed is higher, but with a much simpler algorithm (being the source-position known in VIS approach) and over a limited amount of pixels (those with grey level above threshold).

Ulmer *et al.*²⁰ proposed the use of color-coded targets and the $f \leftrightarrow \infty$ configuration. The advantage of VISdish is the higher accuracy: in the case of OMSoP dish, we obtained 0.1 mrad, but it could be easily enhanced up to 0.01 mrad by adopting a camera with higher bit-depth. A detailed error analysis will be reported in a next paper as soon as the OMSoP dish will be equipped with new facets, better shaped and with higher solar reflectance.

Arqueros *et al.*²¹ proposed the SCCAN method, which is quite similar to VISdish except for using an isolated star as a light source instead of the points/lines displayed by the LCD monitor. In this case, the advantage of VISdish is the full control of the light source position, without any need to modify the orientation of the dish or to wait for the apparent star moving.

ACKNOWLEDGMENTS

The whole activity on VISdish was financed by the E.U. Project No. OMSoP, FP7-308952. We would like to thanks the other partners (KTH Royal Institute of Technology in Stockholm, University City of London, University of Seville, University Roma Tre, Compower, European Turbine Network) for the fruitful collaboration.

We wish to thank Gianremo Giorgi for the excellent mechanical works and Ettore Giovannini for the design.

¹See <http://www.solarpaces.org/csp-technology> for SolarPACES, CSP - How it Works; 2016.

²See <http://www.solarpaces.org/press-room/news/item/98-new-solar-thermal-electricity-report> for Greenpeace International, SolarPACES, and ESTELA, Solar Thermal Electricity Global Outlook; 2016.

³U. Jamil and W. Ali, "Performance tests and efficiency analysis of solar invictus 53s a parabolic dish solar collector for direct steam generation," *AIP Conf. Proc.* **1734**, 070018 (2016).

⁴R. Bader, L. J. Venstrom, J. H. Davidson, and W. Lipiski, "Thermodynamic analysis of isothermal redox cycling of ceria for solar fuel production," *Energy Fuels* **27**, 5533–5544 (2013).

⁵T. Yu, J. Lu, J. Ding, W. Wang, Y. Lu, and Q. Yuan, "Thermochemical storage performance of methane reforming with carbon dioxide tubular reactor in a solar dish system," *Energy Procedia* **75**, 430–435 (2015).

⁶See <https://omsop.serverdata.net/Pages/Home.aspx> for OMSoP, Optimised Microturbine Solar Power system; 2013.

⁷M. Montecchi, see <http://brevetti.enea.it> for Metodo e sistema di ispezione visiva per il controllo di qualita' della forma di riflettori concentratori; 2008.

⁸M. Montecchi, A. Benedetti, and G. Cara, "Optical alignment of parabolic trough modules," in Proceedings of SolarPACES, 2010.

⁹M. Montecchi and M. Dalla Casa, "Post-assembly *in-situ* check of parabolic trough modules by visshed," will be presented at SolarPACES, 2017.

¹⁰M. Montecchi, A. Benedetti, and G. Cara, "Fast 3D optical-profilometer for the shape-accuracy control of parabolic trough facets," in Proceedings of SolarPACES, 2011.

¹¹C. E. Andraka, R. B. Diver, and K. S. Rawlinson, "Improved alignment technique for dish concentrators," *ASME 2003 International Solar Energy Conference, Solar Energy*, 625–635 (2003).

¹²See http://docs.opencv.org/2.4.13/modules/calib3d/doc/camera_calibration_and_3d_reconstruction.html for OpenCV, Camera Calibration and 3D Reconstruction; 2016.

¹³C. E. Andraka, J. Yellowhair, K. Trapeznikov, J. Carlson, B. Myer, B. Stone, and K. Hunt, "Aimfast: An alignment tool based on fringe reflection methods applied to dish concentrators," *J. Sol. Energy Eng., Trans. ASME* **133**, 031018 (2011).

¹⁴W. Li, T. Bothe, C. Von Koplow, and W. Jptner, "Evaluation methods for gradient measurement techniques," *Proc. SPIE: Opt. Metrol. Prod. Eng.* **5457**, 27–30 (2004).

¹⁵M. Montecchi, "Proposal of a new parameter for the comprehensive qualification of solar mirrors for CSP applications," *AIP Conf. Proc.* **1734**, 130014 (2016).

¹⁶M. Montecchi, "Approximated method for modelling hemispherical reflectance and evaluating near-specular reflectance of csp mirrors," *Sol. Energy* **92**, 280–287 (2013).

¹⁷M. Montecchi, "Upgrading of enea solar mirror qualification set-up," *Energy Procedia* **49**, 2154–2161 (2014).

¹⁸Y. Wang, S. Li, J. Xu, Y. Wang, X. Cheng, C. Gu, S. Chen, and B. Wan, "An automatic high efficient method for dish concentrator alignment," *Math. Probl. Eng.* **2014**, 1.

¹⁹S. Ulmer, P. Heller, and W. Reinalter, "Slope measurements of parabolic dish concentrators using color-coded targets," *J. Sol. Energy Eng., Trans. ASME* **130**, 0110151–0110155 (2008).

²⁰J. Xiao, X. Wei, Z. Lu, W. Yu, and H. Wu, "A review of available methods for surface shape measurement of solar concentrator in solar thermal power applications," *Renewable Sustainable Energy Rev.* **16**, 2539–2544 (2012).

²¹F. Arqueros, A. Jimnez, and A. Valverde, "A novel procedure for the optical characterization of solar concentrators," *Sol. Energy* **75**, 135–142 (2003).